Combining 3D Deformable Models and Level Set Methods for the Segmentation of Abdominal Aortic Aneurysms

Derek Magee[1], Andrew Bulpitt[1] and Elizabeth Berry[2]
[1]School of Computing
University of Leeds, Leeds, LS1 9JT,UK
[2]Academic Unit of Medical Physics
University of Leeds, Leeds LS1 3EX
drm,andyb@comp.leeds.ac.uk,e.berry@leeds.ac.uk

Abstract

In this paper we present a system that combines the benefits of 3D deformable models and level set methods for medical volume segmentation. Our 3D deformable model is a very computationally efficient method for segmenting medical volumes, however it is not currently able to segment features, such as renal arteries, that are small relative to the imaging slice thickness used. Level Set methods are an alternative approach to deformable models that re-pose the volume segmentation problem as the calculation of the steady state of an initial value Partial Differential Equation (PDE) system on a regular rectilinear or cubic mesh. The segmentation obtained is parameterised by the zero value level set of this mesh (analogous to an iso-surface). These methods are very computationally expensive, but have the advantage of being able to segment relatively small features such as renal arteries. The problem domain explored in this paper is the segmentation of arterial structures. The results of these segmentations are to be used in the assessment of patient suitability for minimally invasive (keyhole) surgical procedures in patients with abnormal aortic aneurysms.

1 Introduction

An abdominal aortic aneurysm (AAA) is a dilation of the abdominal aorta. AAAs usually increase in size with time, and if left untreated eventually rupture causing catastrophic haemorrhage. An AAA may be treated by conventional surgical methods, but increasingly minimally invasive techniques, where a stent graft is placed in the lumen, are being used. Patient suitability is assessed using CT data and a calibrated projection angiogram - only about 10% of patients are suitable for the keyhole repair. Once a candidate has been assessed as suitable, measurements are made from the same images to determine the key dimensions of the required stent. Our overall aim is to automate both of these stages of image analysis, ensuring that the full 3D nature of the CT is used. In this paper we describe a segmentation aproach that combines the benefits of a 3D deformable model

BMVC 2001 doi:10.5244/C.15.35

[2] (computational efficiency) with the ability of the level sets based approach [11] to segment features that are of the order of a single slice thickness in diameter.

2 Background

2.1 A 3D Deformable Model Based on Triangulated Mesh

Our 3D deformable model has been presented previously [2], however a brief description is presented here. The model is based on a triangulated mesh, the structure of which is continuously refined as the model 'grows' to maintain the resolution required to accurately represent the image data.

The deformation of the model is controlled by a strategy similar to that of the level set approch Malladi et al [10] or Caselles et al [4] based on the curvature of the model surface. At each iteration, a model node i is propagated in its normal direction with speed F , controlled by the model's curvature K_i and the image gradient at the node's current location.

$$F_i = k_i(1.0 - \epsilon K_i) \tag{1}$$

where k_i is the image-based speed term defined as

$$k_i = \frac{1}{1 + |\nabla G_\sigma * f(x_i)|} \tag{2}$$

The expression $\nabla G_\sigma * f$ denotes the image f convolved with a Gaussian smoothing filter. The speed term k acts as a stopping function that has values closer to zero in regions of high gradient and values closer to unity in regions of relatively constant intensity. This approach allows the model to be initialised within the object of interest without the requirement for the model to be close to the desired solution, which is often not practical when segmenting complex 3D objects.

The deformable model uses refinement of the underlying mesh structure to maintain the resolution required to accurately represent the image data during the growth of the model as in [3, 1]. In this work, the criteria for refining the mesh structure are based the homogeneity of the voxels across the deformable model boundary and current resolution of the mesh at that location. Regions of the model surface where voxels normal to the surface demonstrate good homogeneity are marked as poorly fitting, indicating the model can deform further into these regions. The homogeneity of the voxels is defined using the fuzzy affinity approach of Jones and Metaxas [7]. The fuzzy affinity between two voxels c and d is defined [7] as

$$u(c,d) = \begin{cases} w_i h_i(f(c), f(d)) + w_g h_g(f(c), f(d)) & \text{if c}\neq d \\ 1 & otherwise \end{cases} \tag{3}$$

which is the linear combination of the fuzzy intensity h_i and fuzzy gradient h_g affinities with weights w_i and w_g. $f(i)$ is the intensity of voxel i.

$$h_i(f(c), f(d)) = e^{-\frac{1}{2}\left[\frac{\frac{1}{2}(f(c)+f(d)) - m_i}{s_i}\right]^2} \tag{4}$$

$$h_g(f(c), f(d)) = e^{-\frac{1}{2}\left[\frac{|f(c)-f(d)| - m_g}{s_g}\right]^2} \tag{5}$$

where m_i , m_g and s_i , s_g are the mean and standard deviations of the voxel intensities and gradients obtained from the voxels within the surface of the deformable model.

At each stationary model node, the affinity of the voxels along a normal profile to the mesh surface is calculated. If no discontinuity in the affinity of the voxels is found then the model is considered to have a poor fit at this location and the node is marked as poorly fitting. The facets of the model surface that contain the node are then earmarked for refinement as in [3].

2.2 Expected Structure Model

Previously we have used Expected Structure Models (ESMs) [2, 9] to determine the location of features of interest to allow the 3D deformable model to grow into these areas. The model of expected structure is incorporated into the deformable model framework by identifying the regions of the deformable model surface that poorly fit the image data and matching these "hypotheses" to the structure model. The matching process identifies regions that correspond to features of interest such as branching vessels rather than regions caused by noise or adjacent structures within the image data. The information on the expected location and direction of the feature of interest captured in the ESM for each matched region is then used to govern the local adaptation of the deformable model's parameters to allow the continued deformation of the model in these matched regions.

The structure model represents the object by a probability density function (pdf) $p(x)$ of the model parameters. In this work, the pdf is represented by a mixture model [6]:

$$p(x) = \sum_{j=1}^{M} p(x|j)P(j) \tag{6}$$

where P(j) are the mixing parameters. The component densities in this case are represented as multi-variate Gaussian distributions dependent on the means μ and covariance matrices $\mathbf{\Sigma}$ of the input vectors $\mathbf{x}$.

$$p(x|j) = \frac{1}{(2\pi)^{n/2}\,|\Sigma_j|^{\frac{1}{2}}} exp\left\{-\frac{1}{2}(\mathbf{x}-\mu_\mathbf{j})^\mathbf{T}\mathbf{\Sigma_j^{-1}}(\mathbf{x}-\mu_\mathbf{j})\right\} \tag{7}$$

The parameters of the mixture distributions are determined using the Expectation Maximisation algorithm [6]. The mean and standard deviation of each measurement over the entire training set is used to normalise the measurement values.

2.3 Level Set Methods for Image and Volume Segmentation

Level set methods [11] are a type of finite element approach used for the modelling of evolving curves or surfaces. These methods have been widely used in the fields of fluid mechanics and material science for some time and have recently been applied within the field of machine vision for segmentation problems (e.g. [10]). The principal idea behind level set methods is the definition a static, evenly spaced mesh in an image or volume space. The values at each point on the mesh relate to the proximity of the mesh point to an evolving curve or surface with the 'level set of zero' defining the location of the curve or surface (this can be thought of as like a contour line on a map). Mesh points contained within the evolving surface are given negative values and mesh points outside the surface

are given positive values. A 'speed function' for the movement of the curve or surface is defined and mesh values are updated (from an initial value) using a discrete time finite element update as described in equation 8.

$$\psi_{t+1} + F|\bigtriangledown \psi_t| = 0 \tag{8}$$

Where:

$$\begin{aligned} \psi_t &= \text{Matrix of mesh values at time t} \\ F &= \text{The speed function} \\ \bigtriangledown &= \text{A suitable spatial difference operator} \end{aligned}$$

The speed function may be made up of several terms. Typically in segmentation applications three terms are used; a constant 'advection' term (analogous to the inflation force used in some deformable models e.g. [5]), a term based on the curvature of the zero level set and a term based on image or volume information such as edges. Curvature and image based terms are only defined on the zero level set (i.e. on the curve or surface), however these terms must be calculated at each mesh point for the mesh update equation (equation 8). The solution to this is to define a 'global extension' to these terms where the value at any given mesh point is defined as the value at the nearest point on the zero level set.

Level set methods have a high computational cost as the nearest point on the zero level set (which may have arbitrary topology) must be found for each mesh point. Narrow-band extensions to level set methods lower the computational cost of the algorithms by only updating the mesh in an area local to the zero level set. These methods require the mesh to be re-initialised every few timesteps as the zero level set approaches the mesh points that have not been updated. This re-initialisation is in itself computationally expensive, however the overall computational cost over time may be reduced substantially using such methods.

3 Combining 3D Deformable Models with Level Set Methods

Our system combines the 3D deformable model with an efficient level set implementation to produce a segmentation including relatively features, such as the renal arteries, in a realistic timescale (under 2 hours for the complete segmentation on a single entry level PIII processor). This compares with a level set only segmentation that must run for many hours (typically 16-32 hours).

Initial segmentation is performed using the 3D deformable model as described previously [2]. This process currently takes around 10 minutes on an entry level PIII processor. The 3D segmentation is traced onto a set of 2D slices and a fill operation used to determine which pixels lie inside the segmentation. These slices are then converted to a regular 3D rectilinear mesh with points lying inside the segmentation given values of -1 and values lying outside the segmentation given values of +1. From this points lying on the level set may be calculated and the mesh recalculated based on distance from these points as in the narrow band level set approach (see [11]). This process is illustrated in figure 3.1.

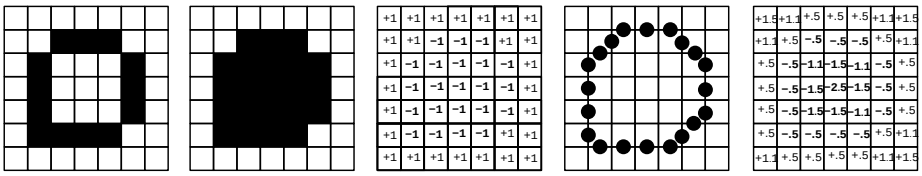

Figure 3.1: An Example of Converting a Deformable Model Segmentation into a Level Set Representation (Only a single 2D Slice is shown)

3.1 Computationally Efficient Volume Segmentation Using Level Set Methods

Voxels from CT data are non cubic due to the nature of the imaging process (the Z voxel dimension is generally larger than the X and Y dimensions). Level Set methods usually use a regular cubic mesh. Level Set methods may be performed on non-cubic rectilinear data by either interpolation of the volume data or taking into account the non cubic nature of the mesh in calculations of distances and derivatives within the mesh. We take the latter approach, due to the lower computational cost involved with this approach.

Narrow band update methods (as described in section 2.3) are used in our implementation. It is useful to note that mesh values may be used to determine how close to the level set the mesh point is and whether it is inside or outside the level set (based on the sign).

Updating only a section of the level set (e.g. 5 slices) at a time makes the recalculation stage of the narrow band method much more efficient. The section to be updated is moved up or down the slices (within a band of interest) after each recalculation stage. This leads to reasonably even 'growth' of the level set within the band of interest. The bands of interest is currently selected by hand, however this process is to be automated in the near future using the Expected Structure Model (ESM).

3.2 Formulation of a Level Set Speed Function from CT Volume Data

The formulation of the speed function is given in equation 9.

$$F(x,y) = (F_0 \bigtriangledown \psi_{x,y} + F_c(x',y') \bigtriangledown \psi_{x',y'}) e^{-F_i(x',y')} \tag{9}$$

Where:

$$\begin{aligned} F(x,y) &= \text{Force at mesh point x,y} \\ F_0 &= \text{Advection force (constant)} \\ x', y' &= \text{Nearest point on the zero level set to x,y} \\ F_c &= \text{Curvature term (concave is +ve)} \\ F_i &= \text{Image force term, based on Gaussian derivative filters} \end{aligned}$$

The image force term F_i is based on a 1D Gaussian derivative filter oriented in the normal direction of the mesh at the point of interest ((x', y')). This filter is preferable

to a simple edge detection such as a Sobel or Canny edge detector as its increased range means that ‘weaker’ edges may be detected. The ‘steerable’ nature of the filter allows calculation of edge strength in the exact direction of interest (rather than extrapolating from x, y and z direction fixed filters). Application in 1D means the computational cost is not high, despite the fact that processing must be performed ‘online’, as normals change from one iteration to the next.

4 Results, Visualisation and Evaluation

Results from the combined automatic segmentation process were compared to interactive segmentations by evaluating the minimum distance between the perimeters of objects in the two segmentations slice by slice (mean, minimum and maximum values of these distances are recorded). Two interactive segmentations were used for each of the four volumes used in this evaluation. Results across the data sets were consistent and, as such, the combined results are given in figure 1. The interactive segmentations for each data set are also compared with each other to give an idea of the robustbustness of this reference technique.

Comparison	Mean	Min	Max
Automatic vs. Interactive	0.57	0	1.16
Interactive vs. Interactive	0.15	0	0.75

All values are in mm

Figure 4.1: Evaluation of Segmentation Accuracy

To put these results in to perspective the diameter of a typical (healthy) Aorta is around 15-20mm. The voxel resolution of the test data sets is between 0.5 and 0.7mm in the slice plane. The results show the automatic segmentation is accurate to within 2 voxels (within the slice plane) and the mean error is nearer 1 voxel.

A useful aspect of 3D segmentations (from the clinical point of view) is that they may be visualised using computer graphics techniques to give increased spatial awareness of the nature of the data set. Figure 2 contains screenshots of the initial and final segmentations visualised using an isosurfacing technique known as marching cubes [8].

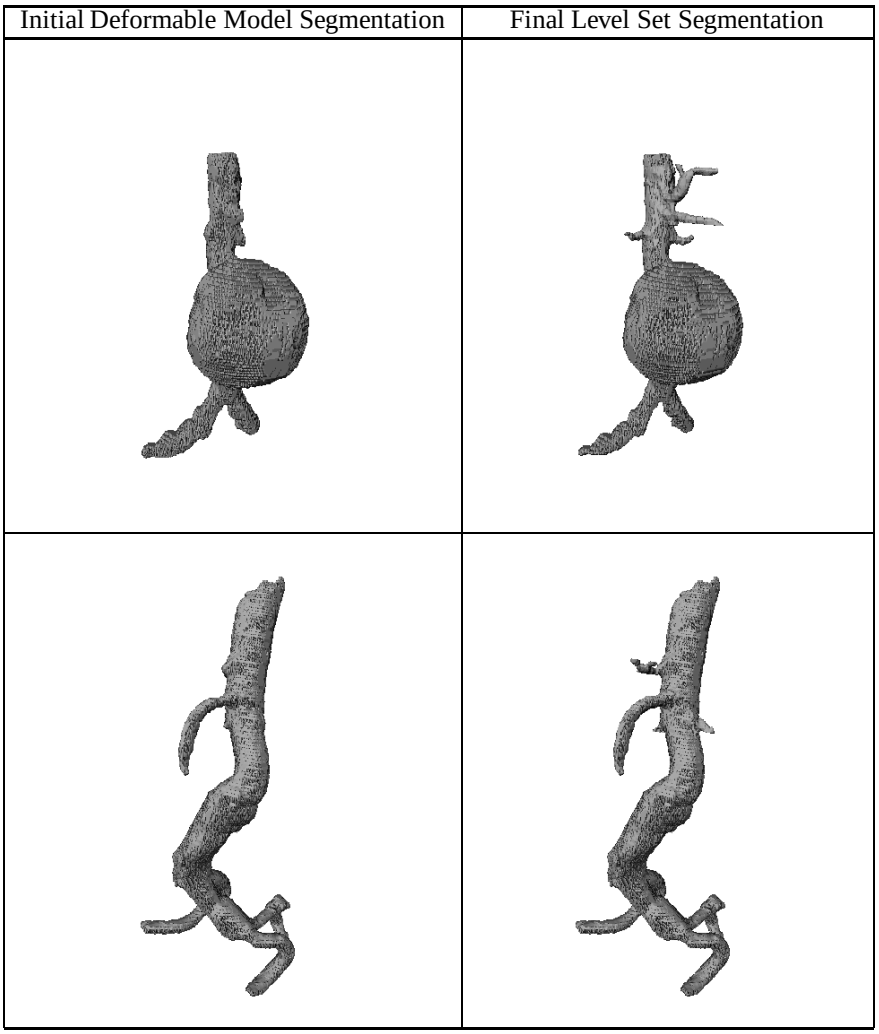

Figure 4.2: Automatic Volume Segmentations Using the Deformable Model and the Combined Method

5 Discussion and Future Work

We have illustrated the various properties of our 3D deformable model (computational efficiency and inability to segment relatively small features) and 3D Level Set Methods (very high computational cost, ability to segment relatively small features). Combining these methods allows segmentation of relatively small, but important, features such as the renal and coliac arteries in a realistic timescale on modest hardware. Determining the location of these features is important in our application as this forms an important part of the information required in the assessment of patient suitability for the keyhole surgical procedure.

As part of our current project we are currently planning a large scale evaluation of our

segmentation techniques. This is required if our automatic segmentation techniques are to replace current interactive segmentations. We have prototyped a desktop system for 2D and 3D visualisation of segmentation results that allows measurements of blood vessel diameters and lengths to be performed easily by surgeons without an invasive procedure (as is currently required). This is currently being further developed in collaboration with the surgical team at St James' Hospital Leeds.

Currently CT volumes are used in patient suitability assessment. In the medium to long term the surgical team wishes to transfer to using MRI as it's imaging medium due to health risks associated with the contrast medium in CT. This offers higher contrast at the expense of spatial resolution. We will evaluate our segmentation techniques on this data when it becomes available.

6 Acknowledgments

The authors are grateful to D.J.A. Scott and D. Kessel for the clinical incentive for the work, to P.J. Dutton for manual segmentations and to C. Craven for image transfer. This work is supported by a grant from the Engineering and Physical Sciences Research Council (GR/M52847) and we acknowledge earlier support from the Wellcome Trust (047635/Z/96/Z).

References

[1] A. J. Bulpitt. Segmentation of complex anatomical structures using 3D deformable models. In *Proc. Medical Image Understanding and Analysis (MIUA'97), Oxford, UK, July 1997*, pages 189–192, 1997.

[2] A. J. Bulpitt, E. Berry, R. D. Boyle, D. J. Scott, and D. Kessel. A deformable model, incorporating expected structure information, for automatic 3D segmentation of complex anatomical structures. In *Proceedings Computer Assisted Radiology and Surgery (CARS2000)*, pages 572–577, 2000.

[3] A. J. Bulpitt and N. D. Efford. An efficient 3D deformable model with a self-optimising mesh. *Image and Vision Computing*, 14:573–580, 1996.

[4] V. Caselles, R. Kimmel, and G. Saprio. Geodesic active contours. *International Journal of Computer Vision*, 22(1):61–79, 1997.

[5] L.D. Cohen. On active contour models and balloons. *CVGIP: Image Understanding*, 53(2):211–218, March 1991.

[6] A. Dempster and D. Rubin N. Laird. Maximum likelihood from incomplete data via the EM algorithm. *Journal of the Royal Statistical Society. Series B*, 39:1–38, 1977.

[7] T.N. Jones and D.N. Metaxas. Image segmentation based on the integration of pixel affinity and deformable models. In *Proc. Conf. Computer Vision and Pattern Recognition (CVPR'98), Seattle, WA, June, 1998*, pages 330–337, 1998.

[8] W.E. Lorensen and H.E. Cline. Marching cubes: A high-resolution 3D surface construction algorithm. *Computer Graphics*, 21(3):163–169, 1987.

[9] D. R. Magee, A. J. Bulpitt, and E. Berry. 3D automated segmentation and structural analysis of vascular trees using deformable models. In *Proceedings IEEE Workshop on Variational and Level Set Methods in Computer Vision*, 2001. To Appear.

[10] R. Malladi, J. Sethian, and B.C. Vemuri. Shape modeling with front propagation: A level set approach. *IEEE Trans. on Pattern Analysis and Machine Intelligence*, 17(2):158–175, Feb. 1995.

[11] J.A. Sethian. *Level Set Methods and Fast Marching Methods*. Cambridge University Press, 1999.